

# Response to Reviewer 2

We appreciate the time and effort that you devoted to reviewing our manuscript and are grateful for the insightful comments on improvements to our paper. We have revised the manuscript accordingly. Below, we provide a point-by-point response to each comment.

**Point 1:** Line 100: Should note that the velocity given is the Doppler Velocity since it is weighted by the backscatter cross section.

*Thank you for the comment. We have revised it in the manuscript.*

*Line 100: For Ka-band radar, the reflectivity factor  $Z$  and the Doppler radial velocity  $V_r$  are calculated from Eq. (5) and (6).*

**Point 2:** Line 104: Does the Haynes et al. algorithm account for the flattening of raindrops as they fall? This would certainly influence the details of the retrievals for heavier rain.

*Thank you for the comment. The algorithm treats liquid hydrometeors as spheres and computes their scattering properties using Mie theory. Thus, the algorithm does not explicitly account for the oblateness (flattening) of raindrops as they fall. We agree that for large drops become more oblate [1]. Yet, in our dataset most precipitations fall in the light to moderate rain regime, the contribution of very large drops is limited. To make this assumption and its implications explicit, we have revised the manuscript and now clarify.*

*Line 304: In addition, the retrievals performance and microphysical characteristics under intense convective conditions are not considered, and raindrops are assumed to be spherical in the radar forward model. Further research is necessary regarding retrievals assumptions in these scenarios with Ka-band zenith-pointing radar, such as the treatment of raindrop shape and DSD parameterizations in the retrieval.*

[1] E. A. Brandes, G. Zhang, and J. Vivekanandan, "Experiments in rainfall estimation with a polarimetric radar in a subtropical environment," *Journal of Applied Meteorology*, vol. 41, no. 6, pp. 674-685, 2002.

**Point 3:** Line 133: It would be useful to see examples of the covarinace matrices or frequency distribution plots of the terms in  $S_a$ .

*Thank you for the comment. We have now added a figure about the frequency distribution of the prior database, a heatmap of  $S_a$ , and a description of prior information in the manuscript.*

*Line 135: The observational vector  $y_{\text{obs}}$  of the optimal estimation algorithm consist of the  $Z$  and  $V_r$  observed by the Ka-band zenith-pointing radar, and the state vector  $x$  comprises  $\log_{10}(N_0)$  and  $D_m$ . The first guess of  $x_a$ , and the priori error covariance matrix  $S_a$  are set based on the prior information of the DSD in Hongyuan. From the precipitation cases described in section 2.1, a subset of 6680*

case is selected to construct the prior dataset. The dataset is obtained by stratified random sampling based on the calculated  $Z$ . This approach reduces the over representation of frequent weak precipitation samples in the prior and yields a more uniformly distributed and representative priori dataset (Boschetti et al., 2016). Then, the values of  $D_m$  are normalized since the state vector are assumed to be approximately Gaussian in optimal estimation, and statistical analysis of the dataset shows that the distribution of  $D_m$  departs from normality. After the transformation, the prior database for the retrieval is established. The mean value of  $\log_{10}(N_0)$  and  $D_m$  in the dataset is set as the first guess  $x_a$  for the retrieval. The frequency distribution of  $\log_{10}(N_0)$  and normalised  $D_m$  are plotted in Figure 2 (a).  $S_a$  calculated from the database are plotted in Figure 2 (b).

Boschetti, L., Stehman, S. V., and Roy, D. P.: A stratified random sampling design in space and time for regional to global scale burned area product validation, Remote sensing of environment, 186, 465-478, 2016.

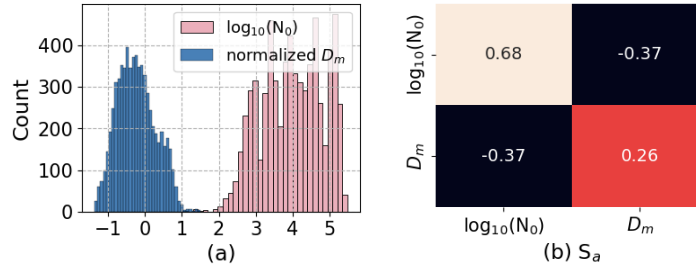


**Figure 2. The frequency distribution of the prior database and the heatmap of  $S_a$  used in the retrieval. (a) Frequency distribution of  $N_0$  and normalized  $D_m$ , and (b) heatmap of  $S_a$ .**

**Point 4:** Line 133: Is the covariance matrix constant or is there a state dependent  $S_a$ ? Are the terms considered to be correlated?

Thank you for the comment. In this study, we use a constant, state-independent covariance matrix  $S_a$  for all retrievals. The off-diagonal terms of  $S_a$  are retained, which represent the priori covariance between  $N_0$  and  $D_m$ . The statistics results of the two parameter has correlation, and using a full  $S_a$  preserves this physically meaningful relationship in the prior. We have added a description in the paper.

**Line 144:** In the study, the  $S_a$  is a constant matrix, and includes correlations between  $N_0$  and  $D_m$  derived from the prior database.

**Point 5 :** Line 134: Additional information should be provided regarding the observational error covariance matrix. Are the errors considered correlated or uncorrelated. What is the source of the uncertainty?

Thank you for the comment. The observational vector is assumed uncorrelated and  $S_y$  is specified as a constant diagonal matrix. The observation uncertainty is 0.5 and 0.5 m/s for  $Z$  and  $V_r$ , respectively. The value on the diagonal of the matrix is the square of observation uncertainty. We have added descriptions on the retrieval method.

*Line 148: The measurement of  $Z$  and  $V_r$  is assumed to be uncorrelated, and the value on the diagonal of the matrix is square of the observation uncertainty.*

**Point 6:** Line 137: There needs to be more information regarding how the terms of Jacobian,  $K_x$ , are calculated and please provide typical examples of the values of  $K_x$ . These details are useful because they show the degree to which the quantities to be retrieved are sensitive to the observations used to constrain them.

*Thank you for the comment. The Jacobian matrix  $K_x$  is defined as  $K_x = \frac{\delta F(x)}{\delta x}$ . We compute the elements of  $K_x$  numerically by finite differences around the current state at each iteration of the retrieval,  $K_x = \frac{\delta F(x)}{\delta x} \approx \frac{F(x + \delta x) - F(x)}{\delta x}$ . In which,  $\delta x$  is a perturbation chosen as 1% for each iterated state vector. we have added a typical example of the values of  $K_x$  in the manuscripts. The typical value of  $K_x$  indicate that the  $Z$  is sensitive to both  $\log_{10}(N_0)$  and  $D_m$ , with  $\partial Z / \partial \log_{10}(N_0)$  and  $\partial Z / \partial D_m$  on the order of 10 and 20, respectively. And  $V_r$  is almost insensitive to  $\log_{10}(N_0)$  and only affected by  $D_m$ , with  $\partial V_r / \partial \log_{10}(N_0) \approx 0$  and  $\partial V_r / \partial D_m \approx 2.3$ . This pattern indicates that the mainly constrains the retrieval of  $N_0$  and  $D_m$ , while  $V_r$  provides complementary sensitivity to  $D_m$ .*

*Line 48: Where  $K_x$  represents the Jacobian matrix computed at the  $x$ -th iteration. The elements of  $K_x$  numerically computed by finite differences around the state vector at each iteration of the retrieval, the perturbation is chosen as 1% of the state vector. The typical value of  $K_x$  indicate that the  $Z$  is sensitive to both  $\log_{10}(N_0)$  and  $D_m$ , with  $\partial Z / \partial \log_{10}(N_0)$  and  $\partial Z / \partial D_m$  on the order of 10 and 20, respectively. And  $V_r$  is almost insensitive to  $\log_{10}(N_0)$  and only affected by  $D_m$ , with  $\partial V_r / \partial \log_{10}(N_0) \approx 0$  and  $\partial V_r / \partial D_m \approx 2.3$ . This pattern indicates that the mainly constrains the retrieval of  $N_0$  and  $D_m$ , while  $V_r$  provides complementary sensitivity to  $D_m$ .*

**Point 7:** Figure 3: The authors should comment on the cause and influence of the systematic biases between the forward calculation and the observations that show up in this plot. the explanation given regarding the height difference and wind may be reasonable but how those issues would result in the biases shown should be demonstrated.

The fact that the calculated values do not lie on the 1:1 line suggest that there may be forward model errors that are not accounted for - i.e. the assumption of spherical raindrops versus reality. Accounting for forward model errors is key in these types of OE inversions. Very often the forward model errors are larger (usually significantly larger) than the uncertainties in the observations.

*Thank you for the comment. In the revised manuscript we provide a more detailed discussion of the systematic differences between the forward-calculated and observed quantities of radar. In section 3.1, we added the discussion on forward model errors.*

*This bias is possibly due to differences in the sampling volumes of the radar and disdrometer, since the disdrometer measures the raindrop at surface and the first effective range bin of radar is at 210m. Besides, the wind at the surface may influence the accuracy of the measurements of the disdrometer. Furthermore, as the raindrops fall, they may deviate from the spherical shape assumption in the radar forward model, leading to discrepancy between the forward simulation and observed values.*

*In section 3.2, we added a discussion on the retrieved and observed  $\log_{10}(N_0)$  and  $D_m$  during the field campaign in July and August 2024.*

*The bias between the retrieved and observed parameters of DSD may be attributed to the observation uncertainties and the differences in the sampling volumes of the two instruments, as well as errors introduced during the fitting of parameters from DSD. More importantly, based on the validation of the radar forward calculation, there is a bias between the radar observation and simulation. Physical assumptions in the scattering calculations, such as the spherical-drop approximation, may also contribute to discrepancies between the retrieved values and the surface DSD parameters.*

**Line 98:** *This bias is possibly due to differences in the sampling volumes of the radar and disdrometer, since the disdrometer measures the raindrop at surface and the first effective range bin of radar is at 210m. In addition, the wind at the surface may influence the accuracy of the measurements of the disdrometer. Furthermore, as the raindrops fall, they may deviate from the spherical shape assumption in the radar forward model, leading to discrepancy between the forward simulation and observed values.*

**Line 230:** *The bias between the retrieved and observed parameters of DSD may be attributed to the observational uncertainties and the differences in the sampling volumes of the two instruments, as well as errors introduced when fitting the DSD parameters. More importantly, based on the validation of the radar forward calculation, there is a bias between the radar observation and simulation. Physical assumptions in the scattering calculations, such as the spherical-drop approximation, may also contribute to discrepancies between the retrieved values and the surface DSD parameters.*

**Point 8:** Figure 4 and 5: Should explain the meaning of the error bars in figures 4 and 5. How are they derived?

*Thank you for the comment. We have added descriptions on the retrieval method. The revised sentence is in italics.*

**Line 45-50:**  $S_x$  in Eq. (11) provides the uncertainty of the retrieved  $x_x$ :

$$S_x = (S_x^{-1} + K_x^T S_y^{-1} K_x)^{-1} \quad (11)$$

*If the convergence of retrieval is achieved, the  $x_x$  and  $S_x$  are the optimal solution  $x_{op}$  and corresponding uncertainty  $S_{op}$*

*Line 213 The final value of  $S_x$  after retrieval convergence is indicated by error bar in the figure.*

**Point 9:** Line 221: The contention made by the authors that  $N_0$  is higher and  $D_m$  smaller at the melting layer is not obvious in the data shown. If the authors think this is important, they should devise a way of showing it more clearly.

*Thank you for the comment. We mean value of  $N_0$  and  $D_m$  are calculated for the lighter and heavier rain, and added a description in the paper.*

*Line 246: Based on the statistic results of lighter rain (maximum value of  $Z$  under 30 dBZ) and heavier rain (maximum value of  $Z$  exceed 30 dBZ) in this day, the retrieved profiles of  $\log_{10}(N_0)$  suggest a higher raindrop concentration in the upper levels of precipitation. At top of the precipitation layer, the mean value  $\log_{10}(N_0)$  is 5.3 for heavier rain and 4.7 for lighter rain, and the mean of  $D_m$  is 0.65 and 0.46 mm. For heavier rain, the vertical variation of the retrieved  $N_0$  and  $D_m$  is larger compared to other precipitation samples, the mean absolute value of  $(Z_{hi+1} - Z_h)/\Delta h$  is 0.01 for  $\log_{10}(N_0)$  and 0.002 for  $D_m$ . For lighter rain, the value of  $\log_{10}(N_0)$  and  $D_m$  is 0.009 and 0.001, respectively. Samples 480 to 500 occurred at the end of a brief rainfall in the morning. The maximum value of  $Z$  is below 20 dBZ. The retrieved profiles of  $\log_{10}(N_0)$  were generally larger than those of other precipitation samples, while the retrieved profiles of  $D_m$  indicated smaller raindrop sizes.*

**Point 10:** Line 242: I wonder if it would make sense to separate this into warm rain events versus cold? It seems likely that the Tsukuba results were associated with rain just below the melting layer when drops derived from large aggregate snow would begin to break up. That is not what is implied by Figure 7 of this paper.

*Thank you for the comment. We agree that distinguishing between warm and cold rain events is important for the characteristic of DSD. A full separation of our statistics into warm and cold rain events would indeed be valuable. Yet this would require accurate classification of each profile and co-located thermodynamic information, which is beyond the scope of the present paper. We have added a paragraph in the discussion to acknowledge this limitation.*

*Line 302: The DSD characteristic of warm and cold rain is an important topic, since it relates to distinct microphysical process. The classification of warm and cold rain event and their DSD characteristic should be studied in future work.*

*In the paper by Tsukuba et al., they refer that some single giant raindrops are observed just below the melting layer. Using this result to compare with the retrieved  $D_m$  parameter here is inappropriate. We have revised this part.*

*Line 269: The mean  $D_m$  for heavy precipitation is generally larger than lighter precipitation, and*

*increases as the raindrops fall, reaching a peak at around 0.5 km. This may relate to the equilibrium of coalescence and breakup effects of raindrops during their falling process (Gatlin et al., 2018).*

Gatlin, P. N., Petersen, W. A., Knupp, K. R., and Carey, L. D.: Observed response of the raindrop size distribution to changes in the melting layer, *Atmosphere*, 9, 319, 2018

**Point 11:** Figure 8: Explain the meaning of the box plot. i.e. Median, Interquartile, 90'th, and 10'th percentiles?

*Thank you for the comment. The central line in each box indicates the median, and the bottom and top edges of the box indicate the 25th and 75th percentiles of the parameters. We have added descriptions on the box plot. The revised sentence is in italics.*

*Line 253: In the box plot, the central line of each box indicates the median, and the box edges indicate the lower and upper quartiles of the parameters.*